This article has been accepted for publication in a future issue of this journal, but has not been fully edited. Content may change prior to final publication. Citation information: DOI 10.1109/TVT.2017.2748988, IEEE Transactions on Vehicular Technology

Comprehensive Modelling to Allow Informed Calculation of DC Traction Systems' Stray Current Levels

C. A. Charalambous, *Member, IEEE.*

***Abstract* — This article is directed towards furnishing stray current modelling on DC traction systems to cope with the variability of a number of influencing parameters. To this end, the archival value of this work is gained by virtue of two new modelling techniques. These new techniques firstly, include a Monte Carlo based approach to take into account the variability of the dominant factors influencing the conductance per unit length between the track and the earth. Secondly, a simulation technique that can provide a more robust representation of the conductance per unit length between the track and the earth coupled with uniform and non-uniform soil models is presented in an attempt to comprehensively assess the levels of stray currents leaving a floating DC traction system.**

***Index Terms* — Stray Current, DC Traction Systems, Resistance to Earth, Corrosion**

I. Introduction

ASSESING stray current interference in DC traction systems entails certain limitations intrinsic to the variability of the parameters and input quantities used in the simulation models. Simulators of different approaches and scales have been reported [1]-[4] in an attempt to investigate the generation and impact of stray currents resulting from the operation of DC rail transit systems. Existing railway stray current model applications have the ability to compute potentials to remote earth and current flow in the modelled components (e.g. rails, supporting and third party infrastructure). These models account for various scenarios dependent upon their design. To this end, almost all simulation models are following semi-deterministic assessment criteria that are derived from bidirectional timetabled train operations, as a function of dynamic changes [5] in multiple train position and train regeneration characteristics [6].

However, DC interference is also liable to a number of other influencing parameters. These are conservatively used to approach mitigation designs or maintenance works. They largely include: a) track's longitudinal conductance, including the impact of wear that will take place during the running of the system, b) conductance per length of the tracks and the other parts of the return circuit (e.g. insulating pads, sleepers, and track slab/mat) and c) soil resistivity of natural ground likely to occur in the field.

These parameters (a-c) usually result from measurements, calculations and assumptions, therefore their quality or state of being determined may be subject to debate. As appropriately described in [7] parameters and input quantities used in estimating the stray current levels, should vary within certain admissible ranges to account for measurement or assumption related uncertainties. These ranges are essential to cope with the lack of knowledge in regimenting the variability of the influencing factors (e.g. environmental conditions, material characteristics and performance) with respect to assessing the DC interference of traction systems during their service operation.

The difficulty in regimenting the variability of the influencing factors has inevitably driven some of the conservatisms built into standards-based approaches. For example, the DC stray current related impacts measured on affected structures and services present the net effect from these variable factors. Current impact assessment approaches are limited to simple time averaging and linear extrapolation of current flows from either static or dynamic model outputs. By contrast current standards (e.g. EN 50122-2 [8] and 50162 [9]) apply criteria based on exceedance of absolute or averaged corrosion potential thresholds without regard to current flows.

Nevertheless, EN 50122-2 [8] explicitly acknowledges that the most important influencing variable for stray currents leaving the tracks is the conductance per unit length between the track and the earth (or alternatively track resistance to earth). Some researchers have employed finite element methods [10]-[13] to comprehensively and more accurately analyze the elements and interfaces (e.g. rails, rail fasteners, and track slab systems) that form the track to earth resistance path for the stray currents to flow. These approaches however, have limited use in large scale simulations since: a) they require extensive computational power and memory capabilities, b) they cannot be conveniently interfaced with the dynamic changes arising from the timetabled train operations and c) they largely assume homogeneous structure and soil characteristics.

C. A. Charalambous is with the Department of Electrical and Computer Engineering, Faculty of Engineering, of the University of Cyprus, PO Box 20537, 1687, Nicosia, Cyprus (e-mail of corresponding author: cchara@ucy.ac.cy).

This article has been accepted for publication in a future issue of this journal, but has not been fully edited. Content may change prior to final publication. Citation information: DOI 10.1109/TVT.2017.2748988, IEEE Transactions on Vehicular Technology

A. *Contributions beyond the State-of-Art*

The focus of the paper is to rationally approach the variability of the dominant factors influencing the conductance per unit length between the track and the earth. To this end, it should be kept in mind that a detailed computer modeling to predict the levels of stray current leaving the tracks generally requires extensive data collection, field work, and subject-matter expertise. Experience on this subject matter suggests that the information regarding the data type and material characteristics of the tracks' supporting and fastening systems can be very limited to stray current control designers. Thus, utilising design or other data in conjunction with simulation models requires an approach that accounts for the uncertainties that may arise in the decision making processes. To this end, the archival value of this work is gained by virtue of the following modelling/techniques' advancements:

- Section II elaborates on a thorough top-down and transparent modelling approach by following Monte Carlo simulation principles. Specifically, the modelling principles employed are generic in nature. They provide the flexibility required to deterministically or probabilistically assess various configurations, defects or uncertainties in the track to earth insulation values; both at the installation and at the operation stages. As an example, this new technique is applied to assess the performance of steel and concrete sleepers on a real DC traction system.
- Moreover, Section III elaborates on an advanced modelling technique, using commercial software [14]. This technique allows the modelling of discrete insulator pats/sleepers along the length of track system rather than assuming that the rails have a uniform resistive coating along their lengths [15]. The latter approach was an inevitable assumption applied in previous models, of such nature, to account for the tracks' resistances to earth values. Thus, the new model is realized through a topologically accurate description of a network of conductors in 3D that can include *both* aboveground conductors and buried conductors. To this extent, it is now possible to robustly investigate the stray current performance of DC traction systems by assuming a more realistic representation of the elements (e.g. insulator pats/sleepers, soil) forming the conductance per unit length between the track and the earth.

II. Model Description for Track to Earth Resistance Calculation

The most important parameter in estimating the stray currents leaving a DC transit system is the rails or track's resistance to earth [8]. If near-perfect insulation was placed around the rails, any level of rail voltage could be tolerated with minimal stray current effects. It should be noted however, that other considerations such as touch voltages restrict the maximum rail potentials allowed in a traction system. The rail resistance (or conductance) to earth is usually a function of the insulating pads/clips, upon which the running rails are mounted. The resistivity of the base material (e.g. ballast) on which the rails are laid is also important. Figure 1 serves the scope of illustrating the physical configuration of the elements forming a fastening system of a single rail.

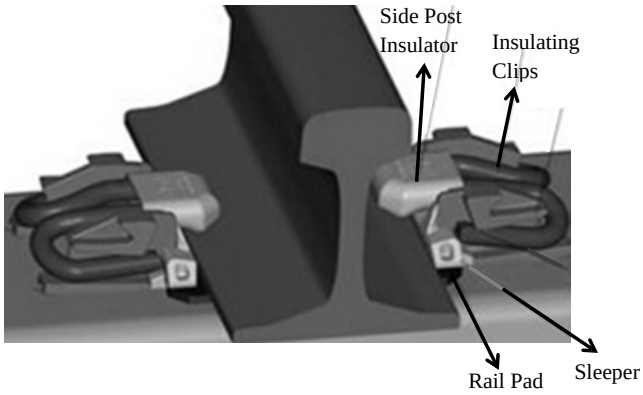

Fig. 1. Physical Configuration of a single Fastening System

Each fastening system provides a spot resistance to earth and depending on the number of fastening systems in a traction system, the Ωkm value of the track-to-earth resistance can be calculated. The spot resistance to earth can be calculated using an equivalent resistive type model, as shown in Fig. 2. This type of model reflects all the elements shown in the physical configuration of a fastening system (Fig.1). It is important to note at this point, that the use of equivalent resistive type models is considered adequate for assessing the stray current leakage density in DC traction systems [8].

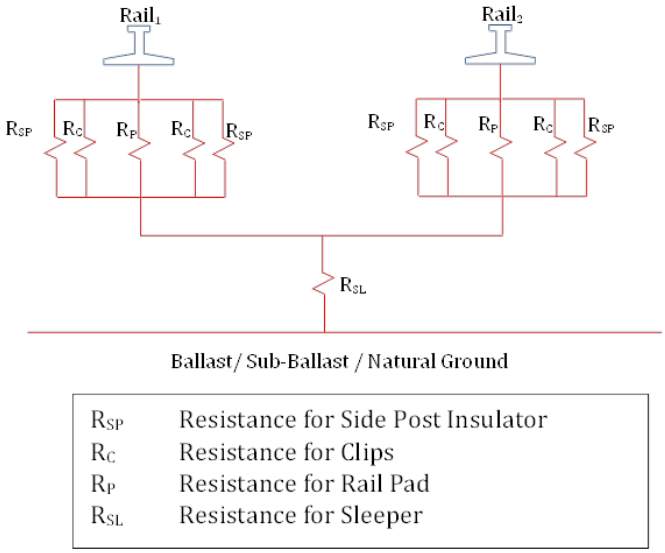

Fig. 2. Equivalent Resistive Type Network for a Single Fastening System

In particular, the resistive type configuration shown in Fig.2 is a generic representation that embraces all elements dominating the resistance to earth value of the track. The same resistive type configuration can be assumed to hold whether the sleepers are, for example, made of concrete or steel, albeit using a different set of data (e.g. for steel, concrete sleepers, insulation fasteners etc.). More precisely, the resistive type configuration shown in Fig. 2 embraces two sets of parallel resistor-branches (R_{SP}// R_C// R_P), one for each rail. The resistors in each branch are used to emulate part of the spot resistance to earth value offered by: a) the two side post insulators, b) the two insulation clips and c) the rail pad. Both branches are electrically connected to a resistor that represents the sleeper (R_{SL}). The latter is used to account for the sleepers' contribution on the resistance between the track and the earth.

This article has been accepted for publication in a future issue of this journal, but has not been fully edited. Content may change prior to final publication. Citation information: DOI 10.1109/TVT.2017.2748988, IEEE Transactions on Vehicular Technology

Nevertheless, the configuration shown in Fig. 2 neglects the resistance of the section of rail between two sleepers, as the rail kilometric resistance can be shown to be much smaller than the resistance between rail and earth for each fastening/sleeper system. Moreover, the resistive network described in Fig.2 can be further coupled with an appropriate soil structure model that characterizes the details of the surrounding track support / foundation and natural ground. This will be discussed in Section III of this paper. Therefore, under the configuration shown in Fig.2, the equivalent spot value of track's resistance to earth $R_{T\text{-}E}$ *(spot)* provided by each sleeper can be calculated as given in (1).

$$R_{T-E}(spot) = R_{SL} + \frac{R_P \times R_{SP} \times R_C}{2\times\{R_C \times R_{SP} + 2\times R_P \times R_{SP} + 2\times R_P \times R_C\}} \quad (1)$$

Moreover, to convert the $R_{T\text{-}E}$ (spot) into a corresponding Ω.km value, it is essential to know the sleepers' spacing value *d*. By using an average spacing value *d*, it is possible to extrapolate the spot value of track resistance to earth to its corresponding $R_{T\text{-}E}$ (Ωkm) value as shown in (2). The $R_{T\text{-}E}$ (Ωkm) value is obtained by considering the contribution that each sleeper/fastener system offers in one kilometre of track.

$$R_{T-E}(\Omega.km) = \frac{R_{T-E}(spot)}{n} \quad (2)$$

Where *n* provides the number of sleepers and fastening systems present in one kilometre of track. The value of *n* can be calculated as given in (3).

$$n = \frac{L}{d} \quad (3)$$

Where *L* is 1000m and *d* is the average spacing between sleepers in 1km section of track.

The electrical equivalent circuit for the calculation shown in (2) would be to assume that the $R_{T\text{-}E}$ (spot) resistors, found in one kilometre, are distributed in parallel. This is graphically illustrated in Fig. 3.

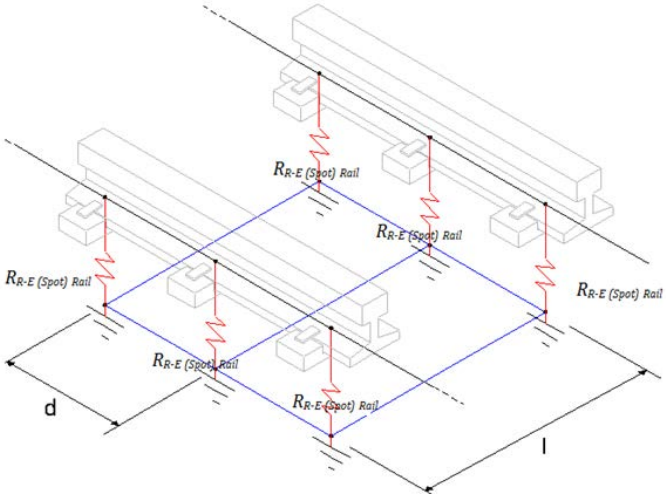

Fig.3. Converting Track-to-Earth Spot Values to Ω.km Values

A. *Case Study*

To facilitate the simulation of the model shown in Fig.2, Table I shows the data as well as the material characteristics deemed necessary for calculating the resistance to earth value of a track system. In particular these data pertain to information received from a real network rail tram project, where new adapted trams will run from a light tram system onto a heavy rail (currently) non-electrified route that benefits from both concrete and steel sleepers [18].

TABLE I
DATA CHARACTERISTICS AND ASSUMPTIONS

Rail	The running rails (e.g. UIC54) are assumed to have longitudinal resistance of 40 mΩ per kilometer. This may be approximately a 19% increase in the nominal longitudinal resistance of 36.3 mΩ per kilometer to account for wear that will take place during the running of the system (cross-sectional area reduction of 16%).	
Rail Pad 	*Type*	rubber pad
	Dimensions (for Concrete Sleeper)	Length:177mm Width:186 mm, Thickness 7.5 mm
	Dimensions (for Steel Sleeper)	Length:177mm Width:186 mm, Thickness 10 mm
	Material (Rubber) Resistivity	1e11-1e16 Ωm (Assumed Values)
Concrete Sleeper 	*Dimensions*	Length: 2515 mm, max width 264 mm, height at rail centre: 203 mm, height at sleeper centre: 140 mm
	Concrete Resistivity	60 Ωm - 200 Ωm (Assumed Values)
	Average Spacing between Sleepers	0.703m
Steel Sleeper 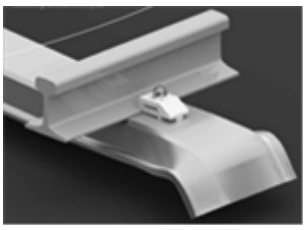	*Dimensions*	Rail seat thickness: 12mm Rail seat width: 160mm Leg thickness: 7 mm Section width: 254mm Section height: 92mm
	Steel Resistivity	Range: 1e-07-7e-07 Ωm (Assumed Values)
	Average Spacing between Sleepers	0.656m
Side Post Insulator & Insulation Clips 	*Material Type and Resistivity*	Assumed Values: E.V.A. (i.e. Ethylene-Vinyl Acetate): ρ = 10^{12} - 10^{17} [Ωcm] E.P.D.M. (i.e. Ethylene Propylene Diene Polymethylene): ρ = 10^{7} - 10^{15} [Ωcm]

This article has been accepted for publication in a future issue of this journal, but has not been fully edited. Content may change prior to final publication. Citation information: DOI 10.1109/TVT.2017.2748988, IEEE Transactions on Vehicular Technology

		Polyamide ρ = 10^{12} - 10^{15} [Ωcm]

volume resistivity of the material, *l* is the thickness and *S* is the contact area of the insulating material.

B. Modelling the Variability of Influencing Parameters

To cope with the variability of the influencing parameters (R_P, R_C, R_{SP}, R_{SL}), the modelling process, for estimating the track to earth resistance values, can be approached probabilistically. These parameters are considered independent and identically distributed, thus the use of Monte-Carlo simulations, is deemed an adequate approach for the scope of this work. Monte Carlo simulations are a problem solving technique which is used to approximate the probability of certain outcomes by running multiple trial runs, using random variables over a specified range. Each random variable is assigned to a specified probability distribution. Thus, for each iteration of the trial process, a random number is drawn from a respective distribution and a calculation takes place. When the required number of iterations is reached, the process is terminated and the results are statistically treated. For the scope of this work, the resistances R_P, R_C, R_{SP}, R_{SL} used in the formulation described in (1) are assigned a normally distributed tolerance with different ranges (expressed in %) around an expected value. The expected value can be calculated when using the known and assumed data illustrated in Table I. Table I shows the data for a fastening configuration benefiting from concrete sleepers and steel sleepers respectively. The whole process followed is shown in Fig. 4. To The process is numerically evaluated by using the data of Table II.

TABLE II
DATA TOLERANCE FOR STEEL AND CONCRETE SLEEPERS' FASTENING CONFIGURATION

Element	Estimated Resistance Value (Ω) - μ	Tolerance - σ (%)
Data Tolerance for Concrete Sleeper Configuration		
*Rail Pad** (R_P)	1.52×10^{11} Ω (for p= 1×10^{12} Ω.m)	Dimensions (W,L,T):±10%, ±10%, ±10%,
		Rubber Resistivity: ±10%
Insulating Clips (R_C)	6.5×10^{7} Ω (assumed value)	±20%
Side Post Insulator (R_{SP})	2.95×10^{6} Ω (assumed value)	±20%
*Concrete Sleeper** (R_{SL})	1295 Ω (for p=180 Ω.m)	Dimensions(W,L,T):±10%, ±10%, ±10%,
		Concrete Resistivity: ±20%
Data Tolerance for Steel Sleeper Configuration		
*Rail Pad** (R_P)	3.04×10^{11} Ω (for p= 1×10^{12} Ω.m)	Dimensions(W,L,T):±10%, ±10%, ±10%,
		Rubber Resistivity: ±10%
Insulating Clips (R_C)	6.5×10^{7} Ω (assumed value)	±20%
Side Post Insulator (R_{SP})	2.95×10^{7} Ω (assumed value)	±20%
*Steel Sleeper** (R_{SL})	1.39×10^{-7} Ω (for p=1.43×10^{-7} Ω.m)	Dimensions(W,L,T):±10%, ±10%, ±10%,
		Steel Resistivity: ±20%

* The expected resistance values for the rail pad and the sleepers can be approximately calculated using the formulation: $R = \rho \times \frac{l}{S}$, where ρ is the volume resistivity of the material, l is the thickness and S is the contact area of the insulating material.

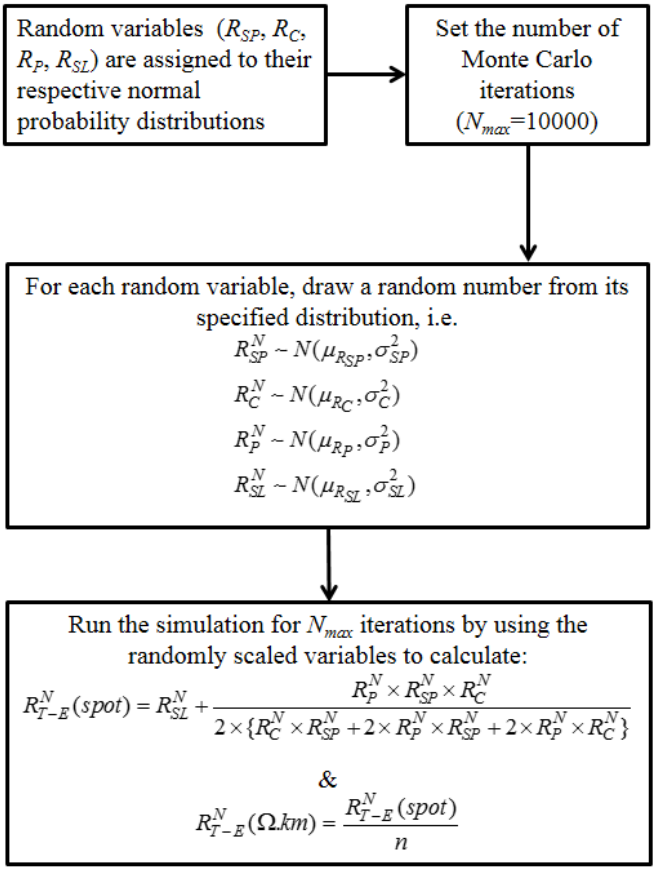

Fig.4. Probabilistic (Monte –Carlo) approach for estimating the track to earth resistance values

C. Numerical Evaluation and Sensitivity Analysis

1) Benchmarking with Measured Data

Following the process described in Fig. 4, the $R_{T-E}^N(spot)$ and $R_{T-E}^N(\Omega km)$ values for the track to earth resistance are evaluates. It is noted that for the $R_{T-E}^N(\Omega km)$ calculation, it is assumed that the number of sleepers in 1km is 1442 and 1524 for the track with concrete and the track with steel sleepers respectively. The evaluation for the steel sleepers' $R_{T-E}^N(\Omega km)$ is shown in Fig. 5 as a box-plot.

With reference to Fig. 5, the results can be interpreted as follows: Following around 10000 Monte-Carlo iterations under the tolerance range specified in Table II, the statistical treatment of the results yielded that the value of the track to earth resistance, under new dry and clean conditions, has 50% probability to lie between 3200 – 3450 Ωkm (Median: 3330 Ωkm). The 25th and 75th can be also seen marked on the plot along with some outlier estimations.

Within Fig. 5, a respective track-to-earth resistance field measurement (in accordance to [18]) is also displayed. This field measurement, in dry conditions on two sections of track that has steel sleepers, has reported the track to earth resistance being 3257 Ωkm. This measurement has been obtained at a section of the track system [19] that is currently

This article has been accepted for publication in a future issue of this journal, but has not been fully edited. Content may change prior to final publication. Citation information: DOI 10.1109/TVT.2017.2748988, IEEE Transactions on Vehicular Technology

not electrified. Of particular note is the fact that the calculated median value (i.e. 3330 Ωkm) conforms to the measured track-to-earth resistance values (i.e. 3257 Ωkm).

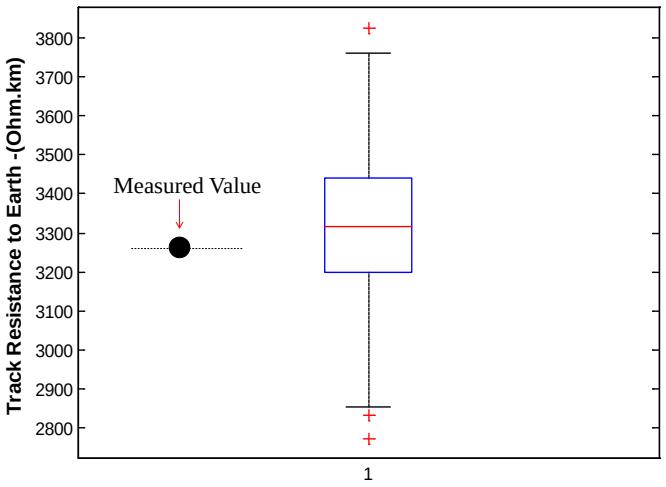

Fig. 5. Resistance to Earth Value of Track with Steel Sleepers $R_{T-E}^{N}(\Omega km)$ – Dry Conditions

2) Embedding the Uncertainties into Stray Current Levels' Calculation

The uncertainties pertaining to the track-resistance to earth values can be further utilized to estimate the overall corrosive stray current levels as given in (4) and (5) for a bonded and floating system respectively.

$$I\_Stray \approx 2 \times \frac{I \cdot r_t \cdot l^2}{2 \cdot R_{T-E}^{N}(\Omega km))} \quad (4)$$

$$I\_Stray \approx 2 \times \frac{I \cdot r_t \cdot l^2}{8 \cdot R_{T-E}^{N}(\Omega km))} \quad (5)$$

In particular, the formulations shown in (4) and (5) can be used to estimate the total stray current levels in a section of track that benefits from two substations at each end (at 0 and at 2km) and a single train located at its midpoint (i.e. at 1km) drawing equal currents from both substations. Where I is the traction return current in A, r_t is the resistance of the track in Ω/km, l is the distance between the train and the two substations and $R_{T-E}^{N}(\Omega km)$ is shown in Fig.6: a) as per the analysis described in Fig. 4 and b) as per the data shown in Tables I and II.

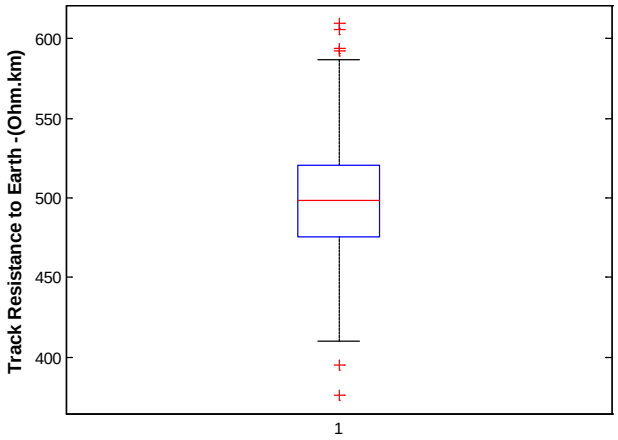

Fig. 6. Resistance to Earth Value of Track with Concrete Sleepers $R_{T-E}^{N}(\Omega km)$

To this extent, Figures 7 and 8 illustrate the total corrosive leakage current anticipated for a bonded and floating system respectively, for varying distances between the two supplying traction substations. The results assume a 1000 A traction return current and a 20mΩ/km resistance of track. A determination of the stray current levels under different traction current return levels can be achieved by applying scaling factors to the modeling results displayed [8].

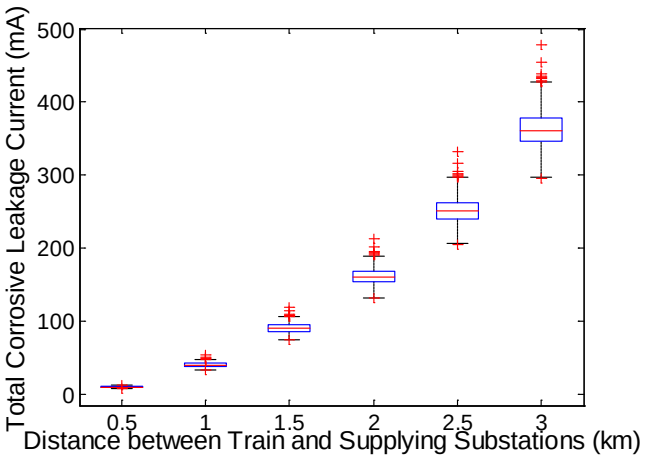

Fig.7. Total Corrosive Leakage Current Level for Different substations Locations – Bonded System

This article has been accepted for publication in a future issue of this journal, but has not been fully edited. Content may change prior to final publication. Citation information: DOI 10.1109/TVT.2017.2748988, IEEE Transactions on Vehicular Technology

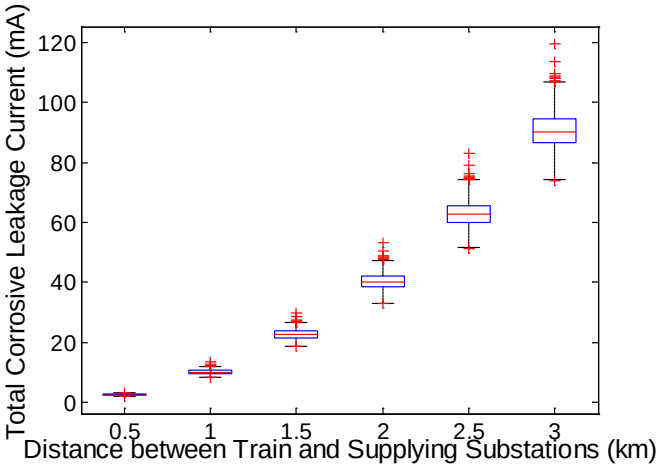

Fig. 8. Total Corrosive Leakage Current Level for Different substations Locations – Floating System

3) Sensitivity Analysis

The first set of sensitivity analysis pertains in investigating the effect of damp that can influence the track's insulation value to earth. To accommodate such an analysis the resistive model shown in Fig. 2, has been modified to the one shown in Fig. 9. It is noted that the following sensitivity analysis is applicable *only* to grounded traction systems, where the running rails are effectively bonded to earth at the substation (e.g. via a stray current collection system).

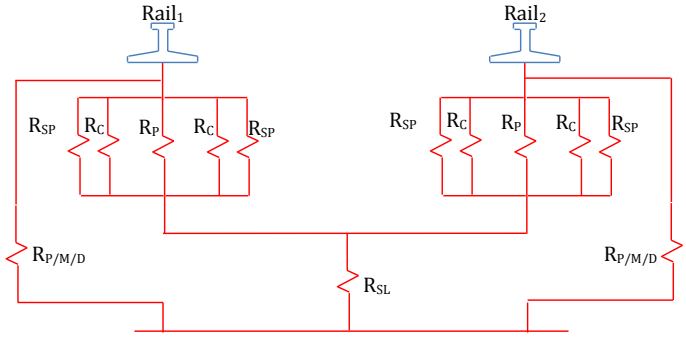

R_{SP}	Resistance: Side Post Insulator
R_C	Resistance: Clips
R_P	Resistance: Rail Pad
R_{SL}	Resistance: Sleeper
$R_{P/M/D}$	Shunt Resistance to Ground for Damp Conditions

Fig.9. Resistive type configuration to estimate the track-to-earth resistance values under damp conditions

As shown in Fig.9, a shunt-resistor ($R_{P/M/D}$) is added in the resistive model in an attempt to simulate the level damp conditions that may take place near or by the track's route. To this end, the sensitivity analysis has considered 9 scenarios which are applied for the case of the track's section that has a concrete sleepers/fastening configuration. The further particulars of these scenarios are shown in Table III. In particular, Scenario 0 simulates new, dry and clean track conditions while Scenario 9 addresses near completely damp track conditions. The latter is simulated by considering an arbitral resistivity value of 2 Ωm. These two scenarios (i.e. Scenario 0 & Scenario 9) are used to set the boundary conditions that would subsequently facilitate the interpolation (10% step change) of the $R_{P/M/D}$ values to account for a in the remaining scenarios (Scenario 2- Scenario 8).

TABLE III
SCENARIOS TO EMULATE DAMP CONDITIONS

Scenario 0	The $R_{P/M/D}$ value is ∞.
Scenario 1	The $R_{P/M/D}$ value is such that decreases the Track-to-Earth Resistance to Earth value (from installation stage) by 10%
Scenario 2	The $R_{P/M/D}$ value is such that decreases the Track-to-Earth Resistance to Earth value (from installation stage) by 20%
Scenario 3	The $R_{P/M/D}$ value is such that decreases the Track-to-Earth Resistance to Earth value (from installation stage) by 30%
Scenario 4	The $R_{P/M/D}$ value is such that decreases the Track-to-Earth Resistance to Earth value (from installation stage) by 40%
Scenario 5	The $R_{P/M/D}$ value is such that decreases the Track-to-Earth Resistance to Earth value (from installation stage) by 50%
Scenario 6	The $R_{P/M/D}$ value is such that decreases the Track-to-Earth Resistance to Earth value (from installation stage) by 60%
Scenario 7	The $R_{P/M/D}$ value is such that decreases the Track-to-Earth Resistance to Earth value (from installation stage) by 70%
Scenario 8	The $R_{P/M/D}$ value is such that decreases the Track-to-Earth Resistance to Earth value (from installation stage) by 80%
Scenario 9	The $R_{P/M/D}$ value is such that decreases the Track-to-Earth Resistance to Earth value (from installation stage) by 90%
** Scenario 0 assumes dry, new and clean conditions i.e. just after installation process.* ***Scenario 9 is considered to emulate near completely damp conditions*	

The simulation results, under the 9 scenarios considered, are shown in Fig. 10. This shows that under near completely damp track conditions (i.e. Scenario 9) the track with concrete sleepers has a 50% probability to have its resistance-to-earth ranging between 42-55 Ωkm.

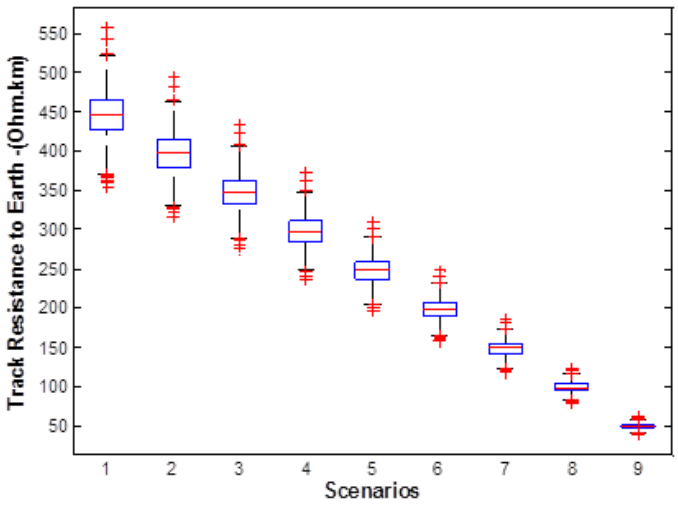

Fig.10. Track Resistance to Earth $R_{T-E}^{N}(\Omega km)$ under Various Scenarios that Emulate Damp Conditions (Track with Concrete Sleepers)

The simulated results for near completely damp condition (i.e. scenarios 8 and 9) are benchmarked (see Fig. 11) against the available field measurements. The field measurements pertain in damp conditions for the section of the track with concrete sleepers [18]. The values of these field measurements were 38 and 97 Ωkm. The simulated median value of $R_{T-E}^{N}(\Omega km)$ in scenario 8 is equal to 98 Ωkm, while the median value of scenario 9 is equal to 48 Ωkm.

This article has been accepted for publication in a future issue of this journal, but has not been fully edited. Content may change prior to final publication. Citation information: DOI 10.1109/TVT.2017.2748988, IEEE Transactions on Vehicular Technology

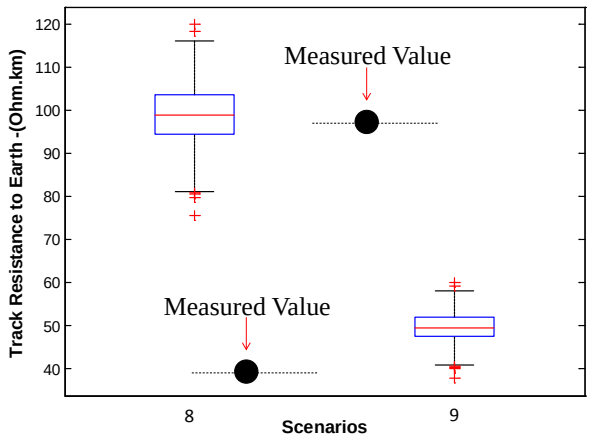

Fig.11. Benchmarking of the Track Resistance to Earth $R_{T-E}^{N}(\Omega km)$ calculations with field measurements

The second set of sensitivity analysis investigates the impact that arises when a certain number of sleeper/fasteners loose or exhibit a decrease of their nominal insulation level during operating conditions. This exercise can be applicable for maintenance related efforts. With reference to Fig. 5, the calculated median value of the track with steel sleepers is 3330 Ωkm, just after the installation process (i.e. under new, dry and clean insulating conditions). This value assumes ideal conditions that suggest that all sleeper/fasteners are performed at their nominal insulation - design values. However, if there is for example a certain equivalent resistance value per kilometre that has to be guaranteed in service (e.g. 3000 Ωkm), we may extract a "permissible" percentage from all sleeper/fasteners (found in 1 km) that is allowed to fall below their nominal insulation design value. The level of "permissible" reduction of their insulation value can be also extracted.

To investigate the concept described just above, a series of simulations has been performed to fulfill the following condition:

- If there is a service resistance to earth value (Ωkm) that has to be guaranteed - how many fasteners/sleepers (present in 1km section of track) can have their insulation conditions being deteriorated and to what extent?

Figure 12 illustrates the results obtained using the track with steel sleepers' configuration as an example. The results can be interpreted as follows. With reference to point B, 20 % of the total sleeper/fasteners that are placed in one kilometre of track are allowed to have a 50 % reduction in their nominal insulation resistance to earth, if a 3000 Ωkm equivalent resistance to earth value per kilometre has to be guaranteed in service. Alternatively, with regard to point A, 32.5% of the total sleeper/fasteners elements that are placed in one kilometre of track are allowed to have a 30 % reduction in their nominal insulation resistance to earth, if a 3000 Ωkm equivalent resistance value per kilometre has to be guaranteed in service.

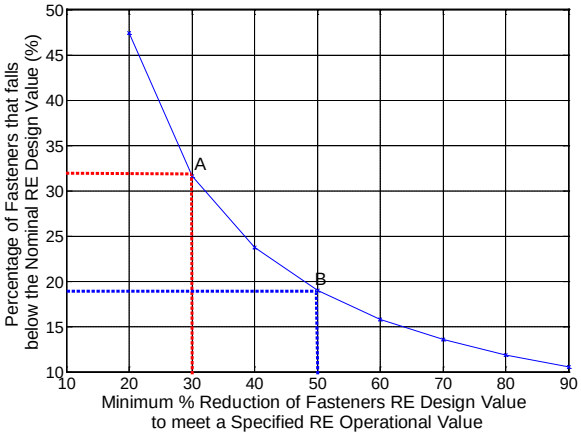

Fig.12. Permissible Reduction of Fasteners Insulation Value to Guarantee a Service Resistance Value per kilometre of 3000 Ωkm (Track with Steel Sleepers)

III. Advanced Modeling to Account for DC Leakage Activity in Floating Traction Systems

The objective of this section is to present a new and more robust modelling approach within commercial software [14] that is able to account for a realistic representation of the elements (e.g. insulator pats/sleepers, soil) forming the conductance per unit length between the track and the earth.

The new modelling approach has the following features:

- The model is realized through a topologically accurate description of a network of conductors in 3D that can include both aboveground conductors and buried conductors. The use of aboveground conductors *advances* any previous modelling endeavours of such nature [4], [15], since the physical position of the rails (i.e. above ground level) is now accurately modelled.
- The latter advancement (i.e. modelling of the physical location of rails accurately) subsequently allows the modelling of discrete insulator pats/sleepers (i.e. fastening systems) along the length of a track system, rather than assuming that the rails have a uniform resistive coating along their lengths.
- It is also possible to couple the fastening systems with an appropriate soil model that characterizes the details of the surrounding track support / foundation and natural ground (i.e. ballast, sub-ballast, subgrade/ natural ground).
- With the above described modelling capabilities, it is possible to model the impact that a failure (or other deteriorating conditions) of the fastening systems have, on the DC leakage activity of floating traction systems.

A. *Description of Simulation Model and Input Parameters*

Figure 13 describes the physical model that is used in the subsequent simulations and analysis. It specifically shows a realistic positioning of the track system (i.e. two rails) relative to the surrounding track support / foundation and natural ground.

This article has been accepted for publication in a future issue of this journal, but has not been fully edited. Content may change prior to final publication. Citation information: DOI 10.1109/TVT.2017.2748988, IEEE Transactions on Vehicular Technology

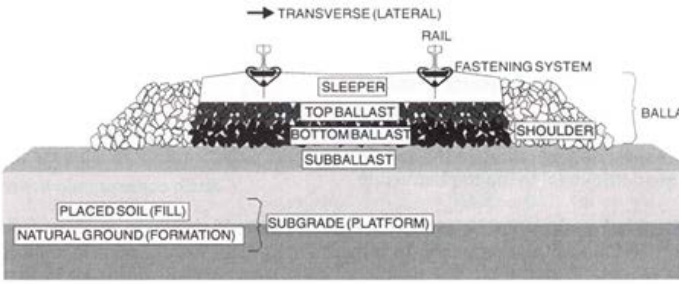

Fig.13. Description of Physical Model

The physical model shown in Fig. 13 is appropriately transferred into a boundary element model (using the HIFREQ module of CDEGS [14]) to simulate the DC stray leakage activity of a floating traction system. The simulation model (both its plan and perspective view) is shown in Fig. 14.

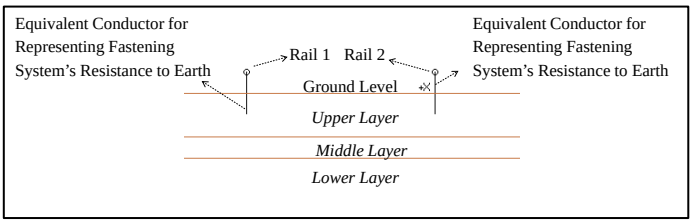

a. Plan Y-Z View

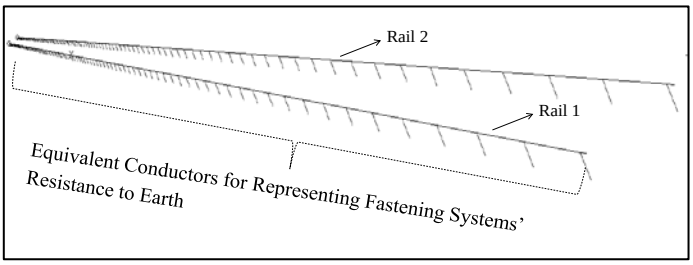

b. Perspective Y-Z View

Fig.14. Description of Simulation Model

The model is designed to simulate the stray current leakage activity of a 1-km section of track when a train draws current from a substation. This 1-km section is representative of a symmetrical 2-km section of track with a single train at the centre and two substations at each end. The current that has been produced by substations at the far end is being drawn by a train placed at midpoint.

Data entry into the simulation model is achieved through a description of a network of conductors in 3D space. HIFREQ module allows both aboveground conductors and buried conductors and the use of multilayer soil structures to be modelled. To this end, a three-layer horizontal soil resistivity structure has been selected, to reflect on the details of the track support / foundation and natural ground shown in Fig. 13. The details of the soil model used are shown in Table IV.

TABLE IV
DESCRIPTION OF REPRESENTATIVE SOIL MODEL

	Description	Resistivity Value (Ωm)	Thickness (mm)
Upper Layer	Sleeper/Ballast	5000 (dry conditions) 180 (wet conditions)	300
Middle Layer	Sub-Ballast	500	150
Lower Layer	Subgrade / Natural Ground	88	infinite

Moreover, Table V tabulates some further base input data and assumptions which are used in the subsequent simulations. It is noted that the data shown in Table V have been calculated to provide an equivalent track conductance (i.e. resistance to earth) of 497 Ωkm. That is to facilitate a valid comparison to the results shown in Fig. 6 that have been produced by the resistive type model described in Section II.

TABLE V
BASE INPUT DATA AND ASSUMPTIONS

Parameter	Description/ Value
System Bonding	Floating
Track length & power supply	1 km single track representative of a 2 km track with a single train at the centre and a supply substation at each end.
Traction Return Current	1000 A to each substation
Rail resistance	40 mΩ/km (UIC54)
Track Resistance	20 mΩ/km (assuming the two rails are bonded)
Length of Equivalent Conductor for Representing Fastening Systems	0.24 m (0.09 m above ground level and 0.15m below ground level)
Resistance of Equivalent Conductor for Representing Fastening Systems' Spot Resistance of Track (Ω/m)	4.1831e5 Ω/m (1.004e5 Ω for 0.24m)
Number of Equivalent conductors in track	202 per km (101 per km per rail)
Equivalent Track conductance (resistance to earth in Ωkm)	$= \frac{4.183\times10^{5}\,\Omega/m\times 0.24m}{202/km} = 497\Omega km$

B. Simulation Results and Analysis

Figure 15 shows the track to earth voltage profile when a train draws current from a substation, assuming a 1-km section of track. This 1-km section can be assumed as being representative of a symmetrical 2-km section of track with a single train at the centre and a substation at each end. The loading conditions assume that a 1000 A is produced by a substation at the far end of track and this is drawn by a train placed at 0m. The results shown in Fig. 15 account both for dry and wet ballast conditions, in an attempt to investigate the impact of surrounding characteristics on the track's voltage to earth. In both cases, the influence of soil structures on the track to earth voltage is negligible. This is expected since the voltage on the track depends merely on the track longitudinal resistance (the track's kilometric resistance is much smaller than the resistance between track and earth). Thus, for every 1mΩ/km of track's longitudinal resistance there will be a resulting voltage drop of 1V/km. For the 20mΩ/km track resistance considered, the resulting voltage difference between the two ends is 20 V. This difference appears on the track as 10 V to remote earth near the train and -10 V to remote earth near the substation, since the track is allowed to float with respect to earth.

This article has been accepted for publication in a future issue of this journal, but has not been fully edited. Content may change prior to final publication. Citation information: DOI 10.1109/TVT.2017.2748988, IEEE Transactions on Vehicular Technology

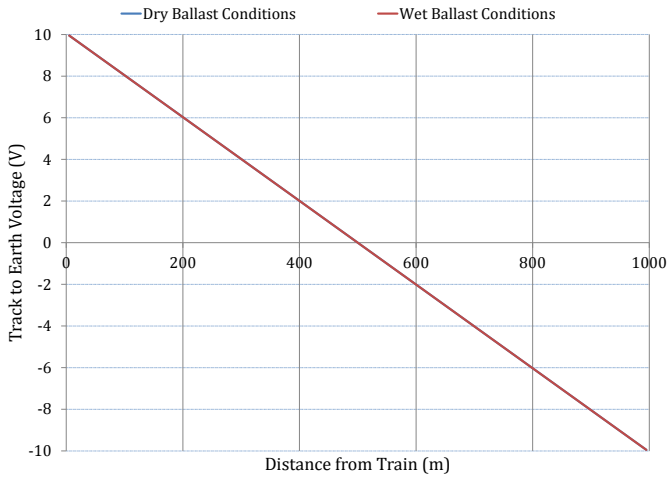

Fig.15. Track to Earth Voltage Profile for a Floating Track System

Although the influence of soil structure is negligible on the track to earth voltage, it appears that the soil structure has some significance on the levels of dc leakage activity to earth. This influence is shown in Fig. 16. In particular, the results reveal that under wet ballast conditions the level of leakage current circulating within the soil may increase significantly. (Note: A positive value in Fig. 16 implies a current leaking out of the track whereas a negative value implies a current leaking back into the track thus completing the current return path).

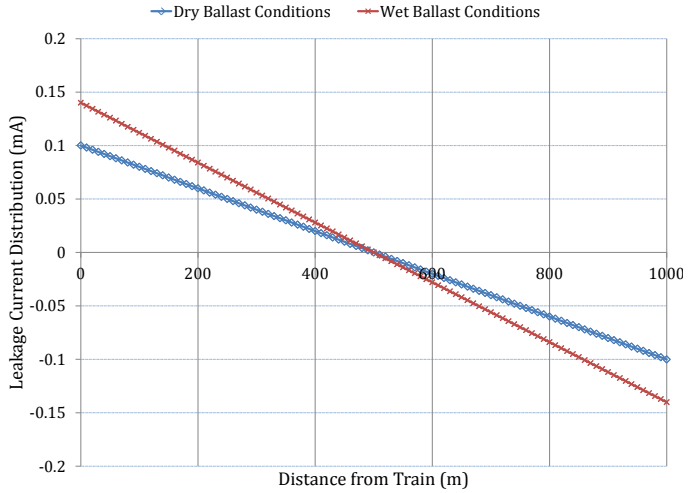

Fig.16. Track to Earth Leakage Current Profile for a Floating Track System

For comprehensively assessing this influence, Table VI benchmarks the total positive (i.e. corrosive) leakage current simulated for each soil model (Fig. 16), as well as the total corrosive leakage current simulated by the resistive type model (see Fig. 8). [Note: The results shown in Fig. 8 suggest that when the distance between the train and the substation is 1km, the median value of the total corrosive leakage current is 10.022 mA and the variance is 46.37 %.] The conclusion drawn from Table VI is that the soil layer near the ground level (i.e. ballast), may have some impact on the level of leakage currents leaving the track, although the track to earth voltage remains unaffected.

TABLE VI
BENCHMARKING OF CUMULATIVE RESULTS

	Total Corrosive Leakage Current (mA)
Resistive Type Model (Section II – Fig. 6)	Median: 10.022 mA Variance: 46.37%
Representative Multilayer Soil Model (Table V – Dry Conditions)	10.206 mA
Representative Multilayer Soil Model (Table V – Wet Conditions)	14.28 mA

1) Simulating Insulation's Failure Conditions in Floating DC Traction Systems

Leakage currents in DC traction systems come as a result of the complete failure of fastening/sleeper systems or from the systematic and inevitable flow of direct current through non-ideal materials of the fastening/sleeper systems. The fastening systems' failure forms an unintentional connection between any current-carrying conductors - which could be the rails (negative bus) with a grounded surface or earth. Such fault conditions can be found in both bonded and floating dc traction systems. The detection mechanisms of these faults depend upon the rails' grounding characteristics and are inevitably different for bonded and floating configurations [16]-[17].

Faults occurring on bonded traction systems are more easily detected and understood. This is due to the presence of a firm reference of the traction system to earth. However, a complete failure of a single fastening system in a floating traction system is less pronounced (or understood) due to the floating nature of the running rails. In fact, a complete failure of a single fastening system intuitively suggests that a dc ground fault has occurred on the negative dc carrying conductor. To understand the arising implication of the latter, one should consider the following remarks:

- In a floating system, a dc ground fault on the negative conductor can be perceived as a "first" ground fault.
- A "first" ground fault on the negative bus will not cause significant fault currents to flow. It is necessary to have a second ground fault on the positive bus to allow large fault currents to circulate through the circuits associated with the two faults - i.e. due to the potential difference established between the two faults' location.
- In floating DC traction systems, it is highly unlikely to have a second ground fault occurrence on the positive bus. This is because a ground fault on the positive bus will be only formed when the overhead contact wire literally falls on the ground.
- Thus, detecting a first ground fault on the negative return conductor of a floating DC traction system is very difficult. This is because there is no distinct potential to ground.

However, excessive leakage currents due to various rails' fastenings failures do exist in floating systems. If this leakage is left undetected or unattended may facilitate a hidden source of accelerated corrosion for supporting and third party infrastructures. Thus, the following simulations serve the scope of demonstrating how leakage current redistribution forms this hidden source of accelerated corrosion.

In the following analysis, insulation failures of the traction system were simulated using the model described in Fig. 14.

This article has been accepted for publication in a future issue of this journal, but has not been fully edited. Content may change prior to final publication. Citation information: DOI 10.1109/TVT.2017.2748988, IEEE Transactions on Vehicular Technology

The failure conditions were simulated by altering the impedance of the equivalent conductor representing the fastening systems' spot resistance from the MΩ to the mΩ range. To this end, Table VII summarises the insulation failure scenarios considered in the analysis.

TABLE VII
DESCRIPTION OF FAULT SCENARIOS

#	Number of Faulted Fastening Configurations	Fault Impedance at each Spot	Fault Location
1	1	0.012 Ω /m	100m
2	1	0.012 Ω /m	800m

Moreover, Table VIII summarises the total positive (i.e. corrosive) leakage current simulated for each scenario examined and benchmarks these against the corrosive leakage current obtained under healthy insulation / dry ballast conditions (see Table VI).

TABLE VIII
SUMMARY OF TOTAL CORROSIVE LEAKAGE CURRENT UNDER FAULT CONDITIONS

#	Total Corrosive Leakage Current (mA)	% Difference Against Healthy Conditions (10.206 mA)
1	10.58 mA	3.67 %
2	10.48 mA	2.70 %

The cumulative results shown in Table VIII suggest that under a single fastening system failure, the level of corrosive leakage current increases slightly. This is expected, since as thoroughly explained above, a single failure/ ground fault on the negative bus of floating systems will not cause significant fault currents to flow. However, it is of particular significance to understand how the leakage current redistributes through the earth to return back to the source. Thus, Figures 17 and 18 show the leakage current redistribution along the length the track under two scenarios. The first scenario pertains in having a single failure, at a location where the track potential is positive with respect to earth (i.e. at 100m). Figure 17 shows that at the failure location there is an approximate 230% increase in the current leaking out of the tracks to the earth. This increase is relative to the leakage current under healthy insulation conditions. The distribution of leakage current in other locations of the track remains fairly unaffected. This local increase however entails a source of local accelerated corrosion risk for the rails.

Fig.17. Track to Earth Leakage Current Redistribution Under Fault Conditions – Scenario 1

Moreover, the second scenario pertains in having a single failure, at a location where the track potential is negative with respect to earth (i.e. at 800m). Figure 18 shows that at the failure location there is an approximate 233% increase in the current returning to the tracks when compared to the current returning under healthy insulation conditions. This suggests that the presence of a ground fault may facilitate the return of more current back to the track, at the location where the single fault had occurred. This intuitively suggests that dc leakage along the track will have a return preference - at the location of the fault. Thus, depending on the fault location, accelerated corrosion risk areas can be framed. A high risk scenario will occur should the dc leakage along the track are picked up on nearby metallic infrastructure as a means to ease their return to their source. Accelerated corrosion will occur at the locations where the current discharges from surrounding metallic infrastructure to return to the source (i.e. track) through the high conductance offered by the single fault to ground.

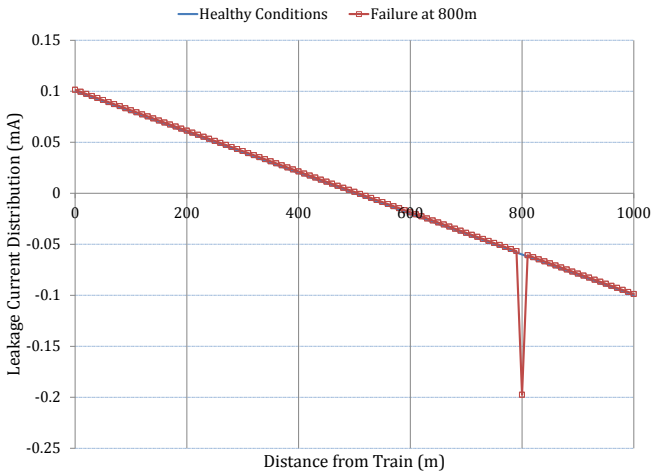

Fig.18. Track to Earth Leakage Current Redistribution Under Fault Conditions – Scenario 1

IV. CONCLUSIONS

Predicting the levels of stray current leaving the tracks requires extensive data collection, field work, and subject-

matter expertise. Information regarding the data type and material characteristics of the tracks' supporting and fastening systems can be very limited to stray current control designers. To cope with the arising uncertainty in estimating: a) the track to earth resistance value and b) corrosive leakage currents, the paper has introduced a probabilistic approach. The influence of soil models that characterize the details of the surrounding track support / foundation and natural ground has been also modelled. The conclusion to this end is that the ballast may have an impact on the level of leakage currents leaving the track, although the monitored track to earth potential remains unaffected. Finally, the paper has presented a series of simulations to provide an understanding on the leakage current redistribution under faulty fastening conditions. The simulations were carried on a floating traction system since the current redistribution is less understood in this type of systems - due to the absence of a distinct potential to earth. The results of these simulations have evidently demonstrated how the leakage current redistribution can form a hidden source of accelerated corrosion on specific locations along the rails and on third party infrastructure - should all necessary conditions are met.

REFERENCES

[1] Ogunsola, A.; Mariscotti, A.; Sandrolini, L., "Estimation of Stray Current From a DC-Electrified Railway and Impressed Potential on a Buried Pipe," *IEEE Tran. Power Del*, vol.27, no.4, pp.2238-2246, Oct. 2012.

[2] C.-H. Lee, "Evaluation of the maximum potential rise in taipei rail transit systems," *IEEE Trans. Power Del*., vol. 20, no. 2, pt. 2, pp. 1379 – 1384, Apr. 2005.

[3] Ogunsola, Ade, Leonardo Sandrolini, and Andrea Mariscotti. "Evaluation of Stray Current From a DC-Electrified Railway With Integrated Electric–Electromechanical Modeling and Traffic Simulation." IEEE Transactions on Industry Applications 51.6 (2015): 5431-5441.

[4] Charalambous, C.A.; Cotton, I.; Aylott, P.; Kokkinos, N.D., "A Holistic Stray Current Assessment of Bored Tunnel Sections of DC Transit Systems," *IEEE Tran. Power Del.*, vol.28, no.2, pp.1048,1056, Apr. 2013.

[5] Charalambous, Charalambos A., and Pete Aylott. "Dynamic stray current evaluations on cut-and-cover sections of DC metro systems." *IEEE Transactions on Vehicular Technology* 63.8 (2014): 3530-3538.

[6] Charalambous, Charalambos A., Ian Cotton, and Pete Aylott. "Modeling for preliminary stray current design assessments: the effect of crosstrack regeneration supply." *IEEE Transactions on Power Delivery* 28.3 (2013): 1899-1908.

[7] J. Bongiorno, G. Boschetti and A. Mariscotti, "Low-Frequency Coupling: Phenomena in Electic Transportation Systems," in IEEE Electrification Magazine, vol. 4, no. 3, pp. 15-22, Sept. 2016. doi: 10.1109/MELE.2016.2584959.

[8] EN 50122-2: "Railway Applications – Fixed Installations – Electrical Safety, earthing and the return circuit – Part 2: Provisions against the effect of stray currents caused by d.c. traction systems", October 2010.

[9] EN-50162-2004; 'Protection against corrosion by stray current from direct current systems' August 2004.

[10] Dolara, A., Foiadelli, F., Leva, S., "Stray Current Effects Mitigation in Subway Tunnels", *IEEE Tran. Power Del*, vol.27, no.4, pp.2304-2311, Oct. 2012.

[11] Zaboli; B. Vahidi; S. Yousefi; M. M. Hosseini-Biyouki, "Evaluation and Control of Stray Current in DC-Electrified Railway Systems," in IEEE Transactions on Vehicular Technology , vol.PP, no.99, pp.1-1 doi: 10.1109/TVT.2016.2555485

[12] Hu, Yunjin, Zhen Zhong, and Jingping Fang. "Finite Element Simulation of Subway Stray Current Field [J]." China Railway Science 6 (2011): 022.

[13] R. J. Hill, S. Brillante and P. J. Leonard, "Railway track transmission line parameters from finite element field modelling: shunt admittance," in IEE Proceedings - Electric Power Applications, vol. 147, no. 3, pp. 227-238, May 2000. doi: 10.1049/ip-epa:20000373

[14] CDEGS Software, Safe Engineering Services & Technologies Ltd Montreal, Quebec, Canada Est. 1978.

[15] I. Cotton, C. Charalambous, P. Ernst and P. Aylott, **"**Stray Current Control in DC Mass Transit S*ystems", IEEE Trans. on Vehicular Technol*., vol. 54, no. 2, pp. 722 – 730, Mar. 2005.

[16] Park, Jae-Do. "Ground Fault Detection and Location for Ungrounded DC Traction Power Systems." IEEE Transactions on Vehicular Technology 64.12 (2015): 5667-5676.

[17] T. Dragičević, X. Lu, J. C. Vasquez and J. M. Guerrero, "DC Microgrids—Part II: A Review of Power Architectures, Applications, and Standardization Issues," in *IEEE Transactions on Power Electronics*, vol. 31, no. 5, pp. 3528-3549, May 2016.

[18] ASTM G165 -99 "Standard Practice for Determining Rail-to-Earth Resistance", 2012

[19] C. A. Charalambous "Modelling to allow comparison of the steel and concrete sleeper performance for a tram train project," Tech. Rep, Intertek UK, May 2015.

ACKNOWLEDGMENT

The work was supported by Intertek UK, under a project based agreement to provide comparison of the steel and concrete sleeper performance for a tram train project in the UK. The provision of the field measurements, by Intertek UK, is sincerely acknowledged.

BIOGRAPHIES

Charalambos A. Charalambous is an Associate Professor, in the Department of Electrical and Computer Engineering, at the University of Cyprus. He is the director of the Power System Modelling Laboratory (PSM Lab). His current research interests include solar applications, DC induced corrosion and control in power system application, earthing/grounding and life-cycle losses evaluation in power system application. Since 2015, he is an active member as an expert in International Standardisation Committee IEC TC/81 Lightning Protection for Structures, Buildings, Persons and Installations. WG11**.**